RESEARCH

Simulation Analysis of Liquid Flow in a Vane-type Surface Tension Tank

Zongyu Wu[1] · Kai Li[2,3] · Wei Han[4] · Guangyu Li[5] · Chengguang Fan[1] · Bingui Xu[6]

Abstract

With the development of space technology, space missions are becoming more and more complex, which puts forward higher requirements for the service life and anti-interference ability of fuel tanks. Due to its lightweight, long service life, and easy processing, the vane-type surface tension tank has been more and more widely used. The vane-type tank enables propellant management with surface tension, however the surface tension is weak. As a result, the control ability of the propellant is limited, which is not suitable for high dynamic maneuvering conditions. This problem limits the development of the vane-type tank and the expansion of mission scenarios. In order to further enhance the propellant management ability of the vane-type surface tension tank, this paper numerically investigated the influence of the T-shaped vane and the perforated vane on propellant management. By applying different boundary conditions, its liquid control ability under complex working conditions is checked. The results show that the T-shaped vane can obviously enhance the liquid transport ability of the tank; the perforated vane can significantly reduce weight, however it weakens the liquid transport ability. The work of this paper can be used to guide the design of the vane-type surface tension tank and has certain guiding significance for the improvement of propellant management performance.

Keywords Simulation analysis · Surface tension tank · T-shaped vane · Perforated vane

Introduction

The vane-type surface tension tank (Jaekle 1991) is an efficient and reliable type of propellant tank. With the help of surface tension, it can realize gas-liquid separation, and then provide gas-free propellant for spacecraft. Due to its light weight and high reliability, it is widely used in satellites, deep space detectors, space stations and so on. For different spacecraft and space missions, vane-type tanks have different structural forms. Before manufacture and use, it is necessary to fully analyze and calculate the flow characteristics of vane-type tank. Its working principle determines that it cannot be verified under the ground experimental conditions. Generally, space microgravity experiment

✉ Kai Li
  likai@imech.ac.cn

✉ Wei Han
  hanwei1984@hotmail.com

  Zongyu Wu
  wuzongyu@nudt.edu.cn

  Guangyu Li
  lgynudt@sina.com

  Chengguang Fan
  chengguangfan@nudt.edu.cn

  Bingui Xu
  xubingui@163.com

1   College of Aerospace Science and Engineering, National University of Defense Technology, Deya Road 109, Changsha 410073, Hunan, China

2   Key Laboratory of Microgravity (National Microgravity Laboratory), Institute of Mechanics, Chinese Academy of Sciences, Beijing 100190, China

3   School of Engineering Science, University of Chinese Academy of Sciences, Beijing 100049, China

4   National Innovation Institute of Defense Technology, Chinese Academy of Military Science, Beijing 100000, China

5   School of Aircraft Engineering, Nanchang Hangkong University, Nanchang 330063, Jiangxi, China

6   Shandong Institute of Space Electronic Technology, Yantai 264003, Shandong, China

(Conrath et al. 2013; Canfield et al. 2013; Hu et al. 2014; Weislogel et al. 2017; Weislogel and McCraney 2019; Hu and Kang 2019) or drop tower experiment (Kulev and Dreyer 2010; Wollman et al. 2016; Chen et al. 2016, 2019; Friese 2019) is often used to study this kind of microgravity fluid phenomenon. However, such experiments are often expensive and difficult to obtain. Numerical simulation is an important means to study and understand the characteristics of the vane-type tank because it is not constrained by experimental conditions.

Researchers have done a lot of important and meaningful work by using numerical simulation technology. Collicott and Weislogel (2002) analyzed the three-dimensional capillary interfaces in spacecraft propellant management devices with the Surface Evolver code. Behruzi et al. (2006) carried out the numerical analyses with the FLOW-3D software to simulate propellant sloshing behavior of the Ariane 5 ESC-A upper stage. Berglund et al. (2007) investigated the sloshing behavior of the liquid hydrogen during the second stage coasting phase of flight with the engineering computational fluid dynamics tool FLOW-3D. Liu et al. (2016) carried out CFD simulation analysis of capillary rise of liquid in Cylindrical container with lateral vanes in space condition. Li et al. (2017) focused on the numerical simulation and analysis of capillary flow under microgravity in fan-shaped asymmetric interior corner. Liu et al. (2020) mainly studied the numerical simulation of the gas-liquid distribution in a vertical vane-type tank with micro downward acceleration. Zhuang et al. (2020) numerically analyzed the fluid transport with parallel guide vanes in a vane-type surface tension tank. Zhang et al. (2020) investigated the influence of the guide vane on liquid transmission performance in a capsule-type vane tank under microgravity by FLOW-3D software. Through years of research, researchers have found that the surface tension, contact angle, and configuration of the channel have a significant influence on liquid flow. In addition, it is also found that the liquid climbing height along vanes under microgravity is proportional to the square root of flow time $\sqrt{t}$. These conclusions are consistent with the experimental phenomena. It can be drawn that the CFD simulation is an effective method to investigate flow phenomena in the fuel tank.

At present, the research mainly focuses on the conventional vane-type tank. In this paper, a special vane-type tank is designed for sounding rocket experiments to explore the influence of T-shaped vanes and perforated vanes on the management characteristics of vane-type tanks numerically, so as to provide basis for the design of vane-type tanks. Next, the conclusion of this work will be verified by sounding rocket test in the future. In "Physical Model", the vane-type tank studied in this paper is described in detail. In "Preprocessing of Numerical Simulation", the relevant preprocessing of numerical simulations are introduced. In "Results and Discussion", the simulation results are analyzed and discussed . This paper is summarized in "Conclusion".

Physical Model

The structure of the vane-type tank is usually simple without moving parts. Considering the difficulty of processing, special-shaped structure is rarely used. Common basic propellant management components include inner and outer vanes, sponges, etc. The inner vane is mainly used for gas-liquid separation of propellant, controlling the gas around the vent tube and the liquid around the discharge port; The outer vane is mainly used to reorientate the propellant. Generally speaking, the common vane-type tank configurations include inner vane-type tank, outer vane-type tank and inner-outer combined vane-type tank. The characteristic of the inner vane-type tank is that it can better realize gas-liquid separation, but it can not reorientate the propellant independently; The outer vane-type tank can quickly reorientate the propellant, but the control ability of the propellant is weak, so it is suitable for tasks with small-acceleration interference; Inner-outer vane-type tanks can not only realize gas-liquid separation, but also quickly realize reorientation, but it increase a certain weight compared with the first two vane-type tanks. In the design stage of the vane-type tank, appropriate configuration should be selected according to the different requirements of the task.

In order to further improve the performance of the vane-type tank, a new experimental vane-type tank for small sounding rocket experiment is designed in this section to test the influence of T-shaped vanes and perforated vanes on the propellant management performance of the vane-type tank. Its configuration is shown in Fig. 1. The inner diameter of the vane-type tank is 12.6 cm and the volume is about 1L. The green parts indicate outer vanes, the gray parts indicate inner vanes and the blue part indicates vent tube. The yellow part is a limit mechanism used to fix the outer vanes. The liquid outlet is located at the bottom of the vane-type tank. Figure 1 simplifies the vane-type tank and omits the liquid outlet and pipelines.

Due to the size limitation of the sounding rocket, it is impossible to arrange multiple fuel tanks for comparison. The experimental vane-type tank adopts the propellant management devices(PMD) shown in the Fig. 2. The experimental vane-type tank is the inner-outer combined vane-type tank, which is composed of two ordinary inner vanes, two perforated inner vanes, three ordinary outer vanes and one T-shaped outer vane. The perforated vane can effectively reduce the weight of the propellant management devices; The T-shaped vane is expected to improve the performance of propellant reorientation and the control ability
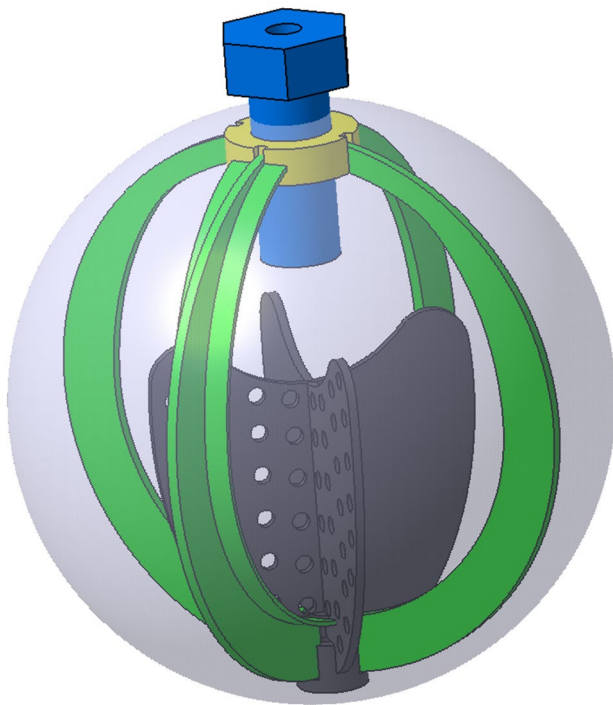
Fig. 1 The structure of the vane-type tank

of propellant. The processing of the perforated vane and T-shaped vane is relatively simple, and there are few space experiment of T-shaped vane at present. The recording and comparison of experimental phenomena can be realized by arranging multiple cameras.

Preprocessing of Numerical Simulation

In this section, the commercial software ICEM CFD is used to grid the calculation domain. Due to the complex internal structure of the vane-type tank, unstructured grid is adopted in this paper. Three meshes with different grid number are

chose to conduct the mesh independence analysis. The grid number of Mesh 1(Corse) is about 550 thousand. The grid number of Mesh 2(Median) is about 940 thousand. The grid number of Mesh 3(Fine) is about 1.92 million. Three meshes are used to simulate the propellant positioning process in the vane-type tank when the filling ratio is 20%. Due to the simulation results of Mesh 2 and Mesh 3 are almost identical, Mesh 2 is adopted in the following simulations to save the computation time. The minimum volume of the grids is $4.360937e^{-13}m^3$. The minimum face area of the grids is $4.74587e^{-9}m^2$. Figure 3 shows the grid distribution of the calculation domain.

To simulate the free surface flow the commercial CFD solver Fluent is used. For two-phase flow problems such as free surface flow, the volume-of-fluid(VOF) method in fluent can better solve these problems. VOF method is an interface tracking method based on Euler grid. In this method, the incompatible fluid components share a set of momentum equations, and the phase volume fraction is introduced to track the interphase interface in the calculation domain. As a result, the VOF method is used to simulate the free surface flow in the vane-type tank.

Before solving, a series of parameters should be set. Due to the liquid flow in the tank belongs to low-speed incompressible flow, the pressure based solver is used to calculate here. Although the density based solver has been expanded into a solution method that can solve a wide flow velocity range, there is no VOF model in the density based solver, which is one of the reasons why the density based solver is not used in the simulation. Set
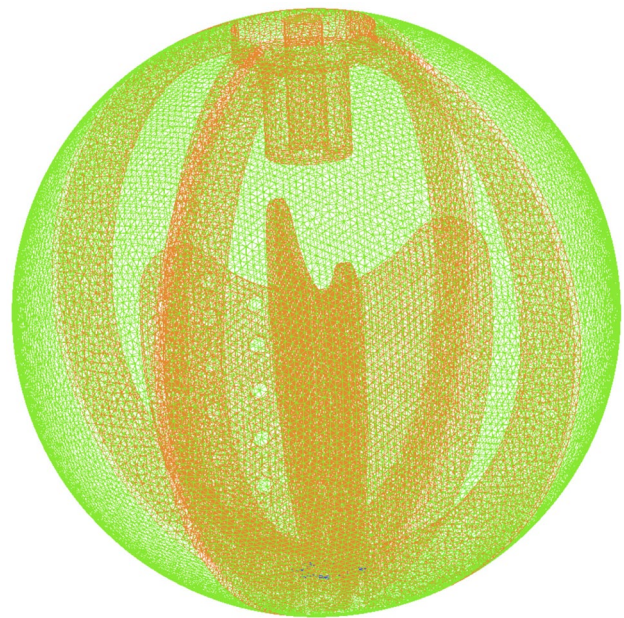

Fig. 2 The propellant management device of the vane-type tank

Fig. 3 The mesh of the vane-type tank

Table 1 The properties of the two phases

Fluid	$\rho(kg/m^3)$	$\mu(kg/(ms))$	$\alpha(°)$	$\sigma(N/m)$
N_2	1.138	1.663e-5	\	\
$C_6F_{15}N$	1736	8.68e-4	0	0.0127

the basic phase as nitrogen(N_2) and the second phase as perfluorotriethylamine($C_6F_{15}N$). The physical properties (density ρ, viscosity μ, contact angle α and surface tension σ) at 20°C of N_2 and $C_6F_{15}N$ are shown in the Table 1.

The tank wall and propellant management devices are set as wall boundary conditions, that is, no penetration and no slip boundary conditions are adopted. In the near wall region, the logarithmic wall function is used to simulate the near wall flow. In addition, the pressure term is discretized by body force weighted method, the momentum term is discretized by QUICK method, the volume fraction term is discretized by GEO-Construct method, and the pressure velocity coupling is discretized by PISO method. The initial gauge pressure is 0 Pa. The initial velocity is 0 m/s. The gravity level is 0g. Finally, the initial volume fraction distribution in the calculation domain should be set according to the specific situation.

Results and Discussion

This section mainly simulates the flow characteristics of propellant during positioning and reorientation in the vane-type tank. Due to there are both gas and liquid in the tank, when the filling ratio of liquid is different, the flow characteristics will be different. In order to understand the liquid flow characteristics under different filling ratios, the representative filling ratios of 20% and 80% are selected to represent the situation of less and more propellant in the tank respectively.

When the orbit control thruster works, the propellant sinks to the bottom under the propulsion acceleration. After the thruster is shut down, the acceleration disappears and the propellant in the tank will be redistributed along the PMD until the equilibrium state is restored. Figure 4 shows the

propellant positioning process when the propellant filling ratio in the vane-type tank is 20%, and the blue area represents the gas-liquid interface. At the initial moment, the liquid is concentrated at the bottom of the tank (below the blue area), and the gas is concentrated on the top of the tank (above the blue area), as shown in Fig. 4. In fact, the acceleration generated by the orbit control thruster is very small, usually 10^{-5}g-10^{-3}g, which is not enough to sink the propellant completely. For convenience, the extreme condition of complete bottom sinking is considered in the simulation analysis. It can be seen from the Fig. 4 that after the orbit control thruster shutting down, the propellant will climb up along the inner vanes, the outer vanes and the tank wall under the action of surface tension. The propellant climbing along the inner vanes stops climbing after reaching the top of the inner vanes. At this time, the propellant at the outer vanes continues to climb until it reaches the top of the tank. The steady state of gas-liquid distribution when the propellant filling ratio in the tank is 20% under zero gravity is shown in Fig. 4. It can be seen that the propellant is mainly distributed along the inner vanes and the outer vanes.

Figure 5 shows the propellant positioning process when the propellant filling ratio in the vane-type tank is 80%. At the initial moment, the liquid is concentrated at the bottom of the tank (below the blue area), and the gas is concentrated on the top of the tank (above the blue area), as shown in Fig. 5. It can be seen that after the orbit control thruster shutting down, the propellant liquid level near the center line of the tank is gradually decreasing until it is basically flush with the top of the inner vanes. Under the action of surface tension, the propellant climbs upward along the outer vanes and converges at the top of the tank to form a closed bubble. Due to the inertia, after the closed bubble is formed, it will move up and down until the surface tension, microgravity and inertia force reach equilibrium. The steady state of gas-liquid distribution when the propellant filling ratio in the tank is 80% under zero gravity is shown in Fig. 5. It can be seen that the gas forms a closed bubble, which is lifted near the vent tube by the inner vanes.

Figure 6 shows the propellant reorientation process when the filling rate is 20%. It is assumed that when the fuel tank
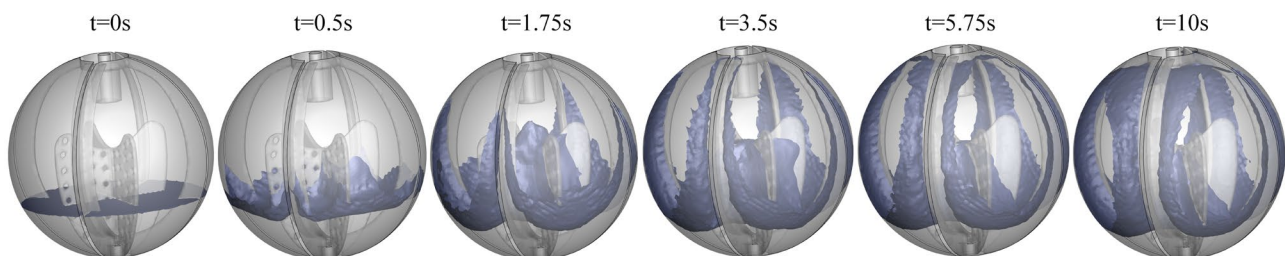
t=0s	t=0.5s	t=1.75s	t=3.5s	t=5.75s	t=10s

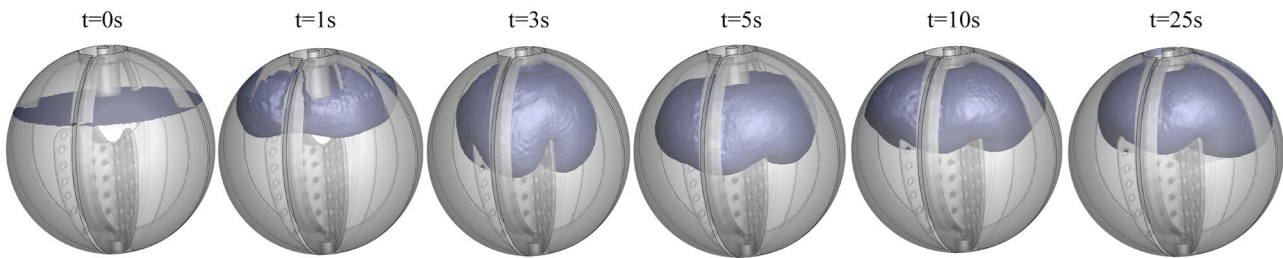**Fig. 4** The liquid positioning process in the vane-type tank when the filling ratio is 20%

Fig. 5 The liquid positioning process in the vane-type tank when the filling ratio is 80%

is strongly disturbed, the propellant is concentrated on the top of the tank and away from the liquid outlet, as shown in Fig. 6, which is an extreme case of propellant distribution in the tank. After the disturbance disappears, the propellant in the tank will be redistributed along the vanes until the equilibrium state is restored. At the initial moment, the liquid is concentrated on the top of the tank (above the blue area), and the gas is concentrated at the bottom of the tank (below the blue area), as shown in Fig. 6. After the disturbance disappears, the propellant mainly flows downward along the outer vanes under the action of surface tension. Until the propellant contacts the inner vanes, then climb up along the inner vanes. The gas-liquid distribution of propellant when it is stable in the tank is shown in Fig. 6.

Figure 7 shows the propellant reorientation process when the propellant filling ratio in the vane-type tank is 80%. At the initial moment, the liquid is concentrated on the top of the tank (above the blue area), and the gas is concentrated

at the bottom of the tank (below the blue area), as shown in Fig. 7. After the disturbance disappears, the propellant flows downward along the inner and outer vanes under the action of surface tension, and a closed annular bubble is formed at the bottom. Under the joint action of the inner and outer vanes, the bubble move upward along the gap between the inner and outer vanes. Due to the annular bubble is unstable, it breaks in the rising process. The gas-liquid equilibrium distribution state is shown in Fig. 7.

Comparison Between the Ordinary Outer Vane and the T-shaped Outer Vane

The liquid transportation performance of T-shaped and ordinary outer vanes under different filling ratios is compared in this section. By processing the simulation results, the liquid climbing distances along the outer vanes can be obtained. Figure 8 shows the comparison of the positioning process of
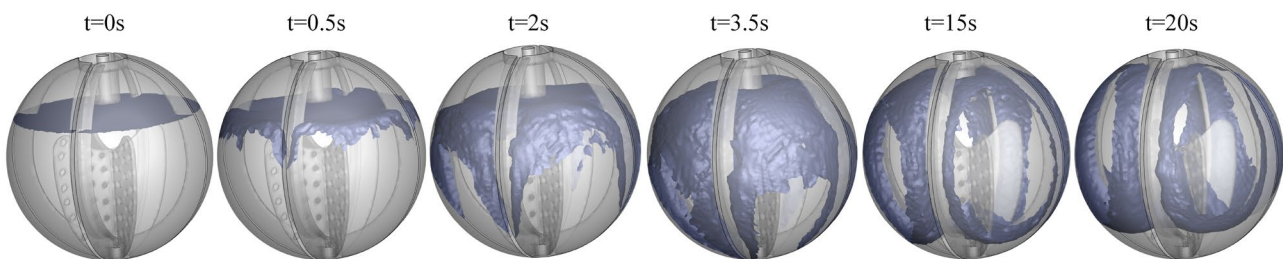

Fig. 6 The liquid reorientation process in the vane-type tank when the filling ratio is 20%
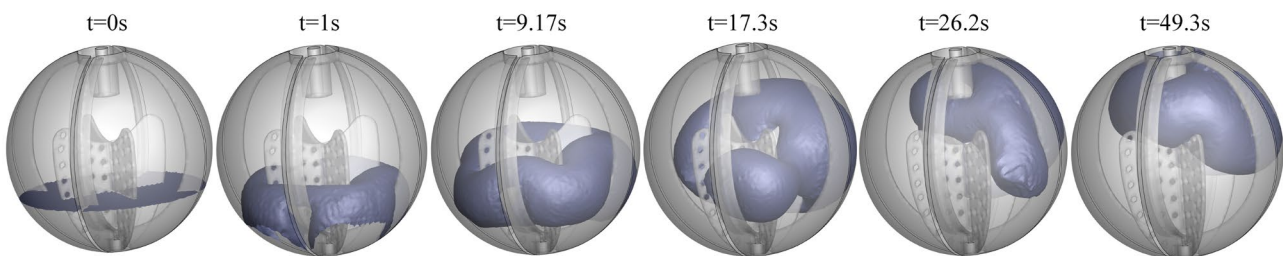

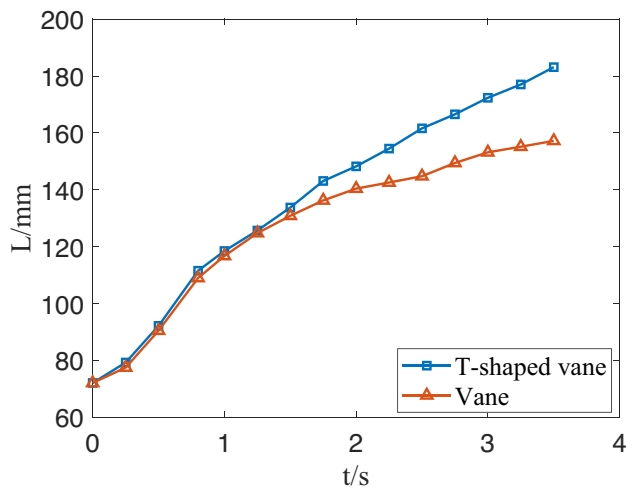**Fig. 7** The liquid reorientation process in the vane-type tank when the filling ratio is 80%

Fig. 8 The comparison of the positioning process of the ordinary outer vane and the T-shaped outer vane when the filling ratio is 20%
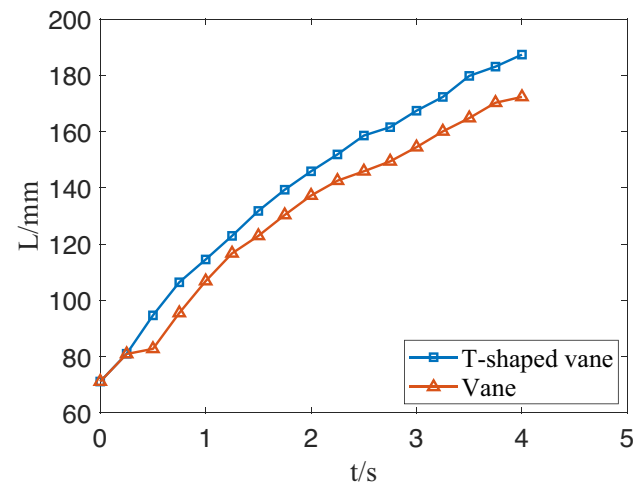

Fig. 10 The comparison of the reorientation process of the ordinary outer vane and the T-shaped outer vane when the filling ratio is 20%

the ordinary outer vane and the T-shaped outer vane when the filling ratio is 20%. Figure 9 shows the comparison of the positioning process of the ordinary outer vane and the T-shaped outer vane when the filling ratio is 80%. Figure 10 shows the comparison of the reorientation process of the ordinary outer vane and the T-shaped outer vane when the filling ratio is 20%. Figure 11 shows the comparison of the reorientation process of the ordinary outer vane and the T-shaped outer vane when the filling ratio is 80%. It can be seen from these figures that the flow of liquid along the T-shaped vanes is faster than that of the ordinary vanes in both the positioning process and the reorientation process. It can be concluded that the T-shaped vanes can accelerate the flow of liquid and enhance the liquid transportation performance.

From the perspective of energy, a system with high energy is unstable, and it always tends to lower its energy to reach a steady state. The liquid surface and the solid surface both have surface free energy. If the liquid can wet the solid surface, the liquid surface free energy is lower than the solid surface free energy; if the liquid cannot wet the solid surface, the liquid surface free energy is higher than the solid surface free energy. The fuel tank material can usually be well wetted by liquid propellant. In the fuel tank the management device will attract liquid to cover its surface, so as to achieve the purpose of reducing the free energy of the solid surface. Assuming the liquid climbs from position L_1 to position L_2, and the energy difference between the two states is ΔE. The T-shaped vanes increase
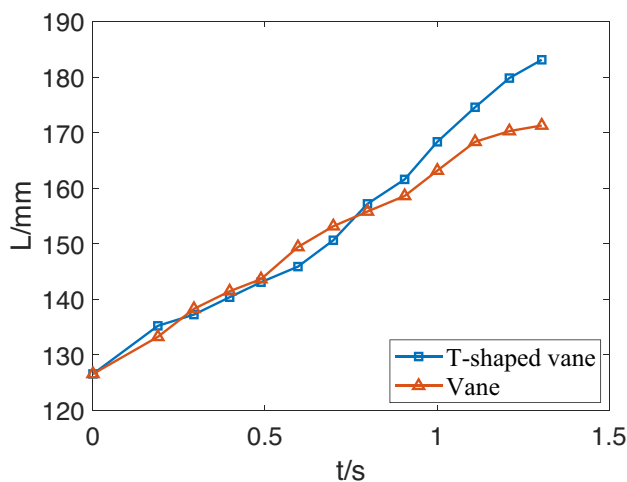

Fig. 9 The comparison of the positioning process of the ordinary outer vane and the T-shaped outer vane when the filling ratio is 80%
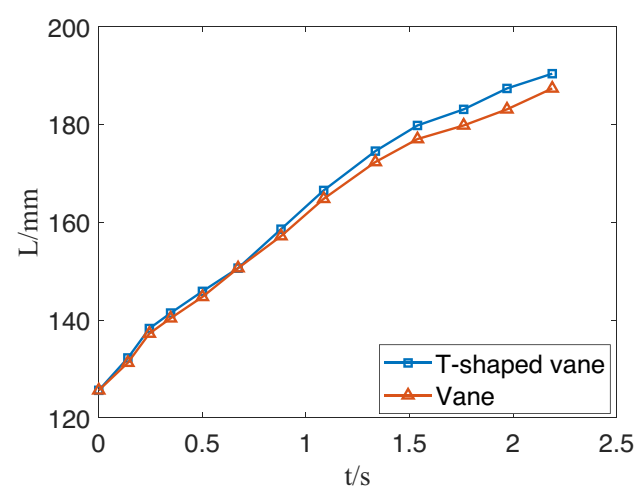

Fig. 11 The comparison of the reorientation process of the ordinary outer vane and the T-shaped outer vane when the filling ratio is 80%

the solid surface area, which in turn increases ΔE. As a result, the liquid will reach L_2 faster.

Comparison Between the Ordinary Inner Vane and the Perforated Inner Vane

The liquid transportation performance of perforated and ordinary inner vanes under different filling ratios is compared in this section. By processing the simulation results, the liquid climbing distances along the inner vanes can be obtained. The liquid flow along the inner vanes can be divided into three categories: Liquid flow between the perforated vane and perforated vane; Liquid flow between the perforated vane and ordinary vane; Liquid flow between the ordinary vane and ordinary vane. Figure 12 shows the comparison of the positioning process of the ordinary inner vane and the perforated inner vane when the filling ratio is 20%. Figure 13 shows the comparison of the reorientation process of the ordinary inner vane and the perforated inner vane when the filling ratio is 80%. It can be seen that the liquid flows fastest between the ordinary vane and ordinary vane, and the liquid flows slowest between the perforated vane and perforated vane. It can be drawn that although the perforated vanes reduce the weight of the tank, it weakens the liquid transportation ability.

From the perspective of energy, drilling on the vanes can obviously reduce the weight, but also reduce the surface area. As a result, the surface free energy reduces, which will slow the liquid flow. Although the perforation reduces frictional resistance to a certain extent, this is not enough to compensate for the reduced performance due to the reduced surface free energy.
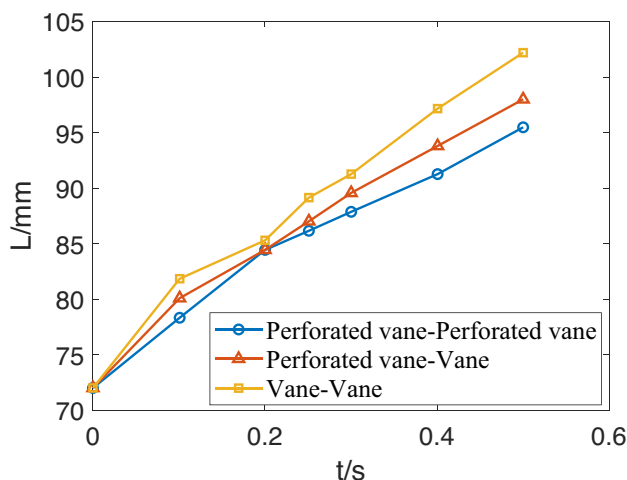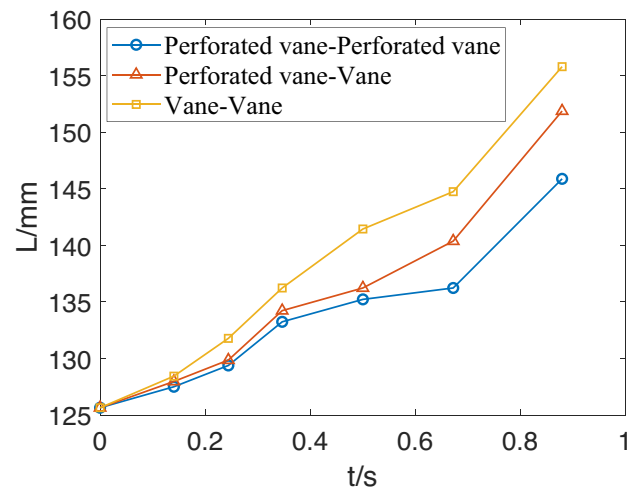

Fig. 13 The comparison of the reorientation process of the ordinary inner vane and the perforated inner vane when the filling ratio is 80%

Conclusion

This paper focuses on the influence of T-shaped vanes and perforated vanes on the propellant management performance of the vane-type surface tension tank. It can be drawn that the T-shaped vanes can accelerate the flow of liquid and enhance the liquid transportation performance. In addition, although the perforated vanes reduce the weight of the tank, it weakens the liquid transportation ability. This work can be used to guide the design of the vane-type surface tension tank. Generally, the T-shaped vane is recommended for tasks with strong demand for liquid transportation ability. In order to reduce the mass of the tank, it can be realized by drilling holes on the vane. The current work is only qualitative. In order to apply the conclusions of this paper to the design of vane-type tanks, further quantitative research is needed, such as the influence of the size of the T-shaped vane, the size of the perforated vanes and the arrangement of holes.

Author Contributions Zongyu Wu, Kai Li and Wei Han wrote the main manuscript text. Guangyu Li prepared Figs. 4–7. Chengguang Fan prepared Figs. 1 and 2. Bingui Xu prepared Fig. 3.

Availability of Data and Material Not applicable.

Fig. 12 The comparison of the positioning process of the ordinary inner vane and the perforated inner vane when the filling ratio is 20%

Declarations

Ethics Approval Not applicable.

Consent to Participate Not applicable.

Consent for Publication Not applicable.

Conflicts of Interest The authors declare that they have no competing interests, or other interests that might be perceived to influence the results and/or discussion reported in this paper.

References

Behruzi, P., Michaelis, M., Khimeche, G.: Behavior of the cryogenic propellant tanks during the first flight of the Ariane 5 ESC-A upper stage. In: 42nd AIAA/ASME/SAE/ASEE Joint Propulsion Conference & Exhibit. American Institute of Aeronautics and Astronautics, Sacramento, California (2006). https://doi.org/10.2514/6.2006-5052

Berglund, M.D., Bassett, C.E., Kelso, J.M., et al.: The Boeing Delta IV launch vehicle—Pulse-settling approach for second-stage hydrogen propellant management. Acta Astronaut. **61**(1–6), 416–424 (2007). https://doi.org/10.1016/j.actaastro.2007.01.048

Canfield, P.J., Bronowicki, P.M., Chen, Y., et al.: The capillary channel flow experiments on the International Space Station: experiment set-up and first results. Exp. Fluids **54**(5), 1519 (2013). https://doi.org/10.1007/s00348-013-1519-1

Chen, S., Han, Z., Duan, L., et al.: Experimental and numerical study on capillary flow along deflectors in plate surface tension tanks in microgravity environment. AIP Adv. **9**(2), 025020 (2019). https://doi.org/10.1063/1.5083672

Chen, X.L., Gao, Y., Liu, Q.S.: Drop tower experiment to study the capillary flow in symmetrical and asymmetrical channels: experimental set-up and preliminary results. Microgravity Sci. Technol. **28**(5), 569–574 (2016). https://doi.org/10.1007/s12217-016-9512-y

Collicott, S., Weislogel, M.: Modeling of the operation of the VTRE propellant management device. In: 38th AIAA/ASME/SAE/ASEE Joint Propulsion Conference & Exhibit. American Institute of Aeronautics and Astronautics, Indianapolis, Indiana (2002). https://doi.org/10.2514/6.2002-4140

Conrath, M., Canfield, P.J., Bronowicki, P.M., et al.: Capillary channel flow experiments aboard the International Space Station. Phys. Rev. E **88**(6), 063009 (2013). https://doi.org/10.1103/PhysRevE.88.063009

Friese, P.S.: Liquid hydrogen sloshing in superheated vessels under microgravity. Exp. Thermal Fluid Sci. **19**, (2019)

Hu, W., Kang, Q.: Physical Science Under Microgravity: Experiments on Board the SJ-10 Recoverable Satellite. Beijing & Springer Nature Singapore Pte Ltd., Science Press (2019)

Hu, W.R., Zhao, J.F., Long, M., et al.: Space program SJ-10 of microgravity research. Microgravity Sci. Technol. **26**(3), 159–169 (2014). https://doi.org/10.1007/s12217-014-9390-0

Jaekle, D. Jr.: Propellant management device conceptual design and analysis - Vanes. In: 27th Joint Propulsion Conference. American Institute of Aeronautics and Astronautics, Sacramento, CA, U.S.A. (1991). https://doi.org/10.2514/6.1991-2172

Kulev, N., Dreyer, M.: Drop tower experiments on non-isothermal reorientation of cryogenic liquids. Microgravity Sci. Technol. **22**(4), 463–474 (2010). https://doi.org/10.1007/s12217-010-9237-2

Li, Y.Q., Cao, W.H., Liu, L.: Numerical simulation of capillary flow in fan-shaped asymmetric interior corner under microgravity. Microgravity Sci. Technol. **29**(1–2), 65–79 (2017). https://doi.org/10.1007/s12217-016-9526-5

Liu, J., Li, Y., Li, W., et al.: Numerical simulation of the flow in a vertical vane type tank with micro downward acceleration. IOP Conference Series: Materials Science and Engineering **793**(1), 012055 (2020). https://doi.org/10.1088/1757-899X/793/1/012055

Liu, X., Huang, Y., Li, G.: CFD simulation of capillary rise of liquid in cylindrical container with lateral vanes. International Journal of Modern Physics: Conference Series **42**(1660), 154 (2016). https://doi.org/10.1142/S201019451660154X

Weislogel, M.M., McCraney, J.T.: The symmetric draining of capillary liquids from containers with interior corners. J. Fluid Mech. **859**, 902–920 (2019). https://doi.org/10.1017/jfm.2018.848

Weislogel, M.M., Chen, Y., Masica, W.J., et al.: Fifty-plus-year post-flight analysis of first fluid experiment aboard a spacecraft. AIAA J. **55**(12), 4042–4052 (2017). https://doi.org/10.2514/1.J055484

Wollman, A., Weislogel, M., Wiles, B., et al.: More investigations in capillary fluidics using a drop tower. Exp. Fluids **57**(4), 57 (2016). https://doi.org/10.1007/s00348-016-2138-4

Zhang, D., Meng, L., Li, Y.Q.: Numerical simulation analysis of liquid transportation in capsule-type vane tank under microgravity. Microgravity Sci. Technol. **32**(5), 817–824 (2020). https://doi.org/10.1007/s12217-020-09811-1

Zhuang, B., Li, Y., Liu, J., et al.: Numerical simulation of fluid transport along parallel vanes for vane type propellant tanks. Microgravity Sci. Technol. **32**(2), 129–138 (2020). https://doi.org/10.1007/s12217-019-09746-2